

# Thermal effects on the mechanical properties of cement mortars reinforced with aramid, glass, basalt and polypropylene fibers

Moosa Mazloom\* and Sajjad Mirzamohammadi

Department of Civil Engineering, Shahid Rajaei Teacher Training University, Tehran, Iran

(Received May 27, 2019, Revised July 16, 2019, Accepted October 1, 2019)

**Abstract.** In this study, thermal effects on the mechanical properties of cement mortars with some types of fibers is investigated. The replaced fibers were made of polypropylene (PP), aramid, glass and basalt. In other words, the main goal of this paper is to study the effects of different fibers on the mechanical properties of cement mortars after subjecting to normal and sub-elevated temperatures. The experimental tests used for investigating these effects were compressive, splitting tensile, and four-point bending tests at 20, 100 and 300°C, respectively. Moreover, the microstructures of the specimens in different temperatures were investigated using scanning electron microscope (SEM). Based on the experimental results, the negative effects of sub-elevated temperatures on four-point bending tests were much more than the others. Moreover, using the fibers with higher melting points could not improve the qualities of the samples in sub-elevated temperatures.

**Keywords:** cement mortars; Polypropylene (PP); aramid; glass; basalt; mechanical properties; thermal properties; sub-elevated temperatures

---

## 1. Introduction

Today, concrete is one of the most frequently used materials in civil engineering. The high compressive strength of concrete makes it suitable for structural applications in the construction industry (Mazloom 2008, Mazloom *et al.* 2004, Mazloom and Ranjbar 2010). However, concrete has a big weak point in tension because brittle cracks appear on it when it is subjected to tensile stresses (Zhang *et al.* 2014, Mazloom and Yoosefi 2013, Salehi and Mazloom 2018, Mazloom and Mahboubi 2017, Mazloom *et al.* 2018a, b). This problem has led to introducing fibers into the world of concrete. The desired results of adding fibers to concrete mixtures are crack reduction, durability improvement, superior ductility, better energy absorption and tensile strength enhancement.

Recently, with the advancement of sciences, fiber reinforced concrete (FRC), high-performance fiber-reinforced cementitious composite (HPFRCC) and cement mortars have been presented. The development and expansion of fiber reinforced concrete (FRC) has undergone many modifications (Li 2007). HPFRCC forms a specific category in fiber-reinforced cementitious composite (FRCC).

It exhibits strain-hardening behavior with multiple cracks before cracking concentration and

---

\*Corresponding author, Associate Professor, E-mail: mazloom@sru.ac.ir; moospoon@yahoo.com

<sup>a</sup> Ms., E-mail: Sajadmirezamohammadi@gmail.com

ultimate fracture (Sirijaroonchai *et al.* 2010). The aim of using high-performance attribute for this material is to separate it from traditional materials.

Engineered cementitious composite is in a unique group of HPFRCC that is based on the theory of micromechanics (Li 2003, 1998, Li *et al.* 2002, Yang and Li 2010, Yang *et al.* 2009). Engineered cementitious composite was first introduced by Li (2007). This material is currently used in pavements, concrete slabs, high-rise buildings and the repair of concrete structures (Qian and Li 2007, Li 2000). The distinctive features of engineered cementitious composite compared to ordinary concrete, fiber reinforced concrete (FRC) and cement mortars are its higher ductility, energy absorption capacity and durability. Furthermore, the strain-hardening behavior and multiple micro-cracks of engineered cementitious composite are its most important features (Li 2012). The materials used for engineered cementitious composite are often polymer fibers such as polyvinyl alcohol (PVA) or polyethylene (PE) ones, silica sand, cement, silica fume, fly ash, water and water reducing admixture. PVA fibers often used in 2% volume content with the length of 8 or 12 mm, which makes this composite have self-consolidation and shotcreting ability.

Many studies have been carried out on modifying the components of cement mortars, including changes in cement matrix components and modifications in the type of fibers. Some researchers have examined the behavior of cement composite reinforced with different percentages of short steel fibers (Li *et al.* 1996). In another study, the performance of cement composite with polyethylene and steel fibers was tested under tensile and dynamic loadings (Maalej *et al.* 2005). In addition, durability tests have been carried out on engineered cementitious composite and cement mortars including chloride (Sahmaran *et al.* 2011a), high alkalinity (Li 2008) and freeze-thaw exposures (Sahmaran and Li 2007). In another study, the mechanical performance of cement composite having PVA fibers with a high amount of fly ash at various temperatures was investigated. The compressive strengths of all the specimens decreased at 200°C; however, they retained their strain-hardening behavior (Yu *et al.* 2015).

This study focuses on the thermal effects on the mechanical properties of cement mortars. Yu *et al.* (2014) and Sahmaran *et al.* (2011b) indicated that the physical and chemical properties of cement paste changed at 200°C and decreased its mechanical properties. The fibers used in cement composites are often polymer fibers (PVA, PE, PP), which their melting points are less than 200°C. This issue can limit the use of cement composites or cement mortars at high or sub-elevated temperatures (Sahmaran *et al.* 2010). The fibers used in this research were polypropylene (PP), aramid, glass and basalt. It is worth noting that PP had the low melting point of 160°C. Also, the melting points of basalt, aramid and glass fibers were 600, 800 and 1400°C, respectively. In fact, the effects of fiber types on the mechanical and thermal properties of cement mortars have been studied in this paper.

## 2. Experimental program

The experimental programs consisted of two phases. In the first one, the effects of PP, aramid, basalt and glass fibers on the mechanical properties of cement mortars were investigated. For this purpose, all the samples had the same mix proportions, and only their fiber types were different. In the second phase, the effects of sub-elevated temperatures on the mechanical properties of the specimens were studied. Further, cement mortars without fibers used as control group.

Table 1 Mix proportions of cement mortars

Cement (kg/m <sup>3</sup> )	850
Silica fume (kg/m <sup>3</sup> )	160
Silica sand (kg/m <sup>3</sup> )	588
Water (kg/m <sup>3</sup> )	390
HRWRA (kg/m <sup>3</sup> )	16.5
Fiber* (kg/m <sup>3</sup> )	18.2
W/(C+SF)	0.38

\*\* PP, Aramid, Basalt, and glass

### 2.1 Material and specimen preparation

The mix proportions used for this paper were based on a mixture of cement composite with some changes to fit the local materials (Yu *et al.* 2018). The details of the mix proportions for all fiber types are given in Table 1. The cementitious materials used for cement mortars were silica fume (SF) and ordinary Portland cement (OPC). It is of note that silica fume is an extremely reactive cementitious material that can be used for the creation of secondary hydration products (Mazloom and Miri 2017, Afzali Naniz and Mazloom 2019, Mazloom *et al.* 2017). The chemical compositions of the cementitious materials are given in Table 2. The silica sand utilized as the aggregate in this research had the maximum and minimum grain sizes of 250  $\mu\text{m}$  and 130  $\mu\text{m}$ , respectively. Polycarboxylate-Based high-range water reducing admixture (HRWRA) was used in the mixes to achieve the desired rheology of the fresh cement mortars. For setting equal conditions, the volume content values of aramid, glass, basalt, and polypropylene fibers were all 2%. Table 3 presents the geometrical and mechanical properties of the fibers.

Table 2 Chemical composition of cement and silica fume

	OPC	SF
SiO <sub>2</sub>	21.30	96.4
CaO	63.48	0.49
Al <sub>2</sub> O <sub>3</sub>	5.13	1.32
Fe <sub>2</sub> O <sub>3</sub>	3.47	0.87
Na <sub>2</sub> O	0.23	0.31
MgO	2.51	0.97
P <sub>2</sub> O <sub>5</sub>	-	0.16
SO <sub>3</sub>	1.67	0.10
K <sub>2</sub> O	0.56	1.01
SiC	-	0.5
C	-	0.3
CL	-	0.04
H <sub>2</sub> O	-	0.08

Table 3 Properties of fibers

Fiber type	Diameter, $\mu\text{m}$	Length, mm	Tensile strength, MPa	Modulus, GPa	Density, $\text{Kg/m}^3$	Melting point, $^{\circ}\text{C}$	Aspect ratio ( $L_f/d_f$ )
Aramid	12	10	3150	80	1440	800	833
Basalt	11	10	2950	90	2670	600	909
Glass	20	10	3450	69	2550	1400	500
PP	23	10	400	2.7	910	165	434

Table 4 Specimen number for each mix proportion

Temperature, $^{\circ}\text{C}$	20	100	300
Compressive strength test	3	3	3
Uniaxial tensile test	3	3	3
Four-point bending test	3	3	3
SEM	1	1	1

Initially, the silica sand and the whole fibers were transferred to the mixer and mixed for 5 min. Then, the cementitious materials were added from fine to coarse-grained order (silica fume-cement) and mixed for 1 min. Finally, water and water reducing agent were added and mixed for 3 min.

The fresh cement mortars were poured into the molds and protected with plastic sheets. After 1 day, the samples were demolded and cured for 27 days in a water tank with the temperature of  $20\pm 2^{\circ}\text{C}$ . Except for the temperature of  $20^{\circ}\text{C}$ , all the samples were heated in a furnace to the mark temperatures of 100 and  $300^{\circ}\text{C}$  for 1 h at a heating rate of  $10^{\circ}\text{C}/\text{min}$ . Then, the specimens were exposed to room temperature and cooled naturally. Moreover, no color change or cracking appeared in the specimens. Furthermore, number of the specimens are shown in Table 4.

## 2.2 Test set up and procedures

### 2.2.1 Compressive test

To determine the compressive strengths of the samples, the ADR Touch device made in the UK was used. The dimensions of the samples were  $15\times 15\times 15\text{ cm}^3$  according to BS 1881: part 108: 1983 (BS 1983a). Additionally, the loading rate was equal to  $0.3\text{ MPa/s}$  based on BS 1881: part 111: 1983 (BS 1983b).

### 2.2.2 Splitting tensile test

Splitting tensile test (ADR Touch device) was carried out to determine the tensile strength of the samples. The samples used for this test were cylinders with dimensions of  $20\times 10\text{ cm}^2$  based on BS 1881: part 117: 1983 (BS 1983c). In addition, the loading rate was equal to  $0.02\text{ MPa/s}$  according to BS 1881: part 117: 1983 (BS 1983c).

### 2.2.3 Four-point-bending test

The device utilized to investigate the flexural behaviors of the samples was Zwick Roell made in Germany. As shown in Fig. 1, this test was done on the samples with dimensions of  $35\times 10\times 10$

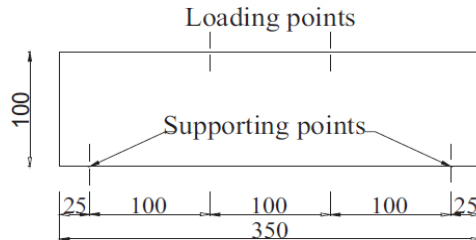


Fig. 1 Sketch of the beam used in the four-point bending test (dimensions: mm)

cm<sup>3</sup> (length, width, depth) in accordance with standard ASTM C1609 (ASTM C1609/M-05 2006). Moreover, the loading rate was 0.5 mm/min (Mazloom *et al.* 2015). It is worth mentioning, in this paper the displacement from the machine used to measure the deflection. However, for measuring exact parameters such as fracture energies should use LVDT (Salehi and Mazloom 2019a, b, Karamloo *et al.* 2017).

#### 2.2.4 Scanning electron microscope (SEM)

In this paper, the microstructures of the samples were investigated using a scanning electron microscope (SEM). For this purpose, the phenom prox device made in the Netherlands was used. The small samples of each mix proportion at any temperature were selected and prepared to be tested.

### 3. Results and discussion

#### 3.1 Compressive properties

The average compressive strengths of the samples at three temperatures of 20, 100 and 300 °C are shown in Fig. 2. The greatest average compressive strength at each temperature was related to the samples containing aramid fibers. The average compressive strength of them at 20, 100 and 300°C was equal to 69.02, 72.09 and 72.52 MPa, respectively. In addition, the minimum average compressive strength at 20, 100 and 300°C was related to the samples having basalt fibers with the value of 52.27, 48.6 and 46.72 MPa, respectively. As can be seen in Fig. 2, the average compressive strength of the samples containing PP fibers was increased by 12.5% and 14% after exposure to 100 and 300°C, respectively. Finally, the average compressive strength of the samples containing glass fibers was increased by 6% at 100°C and decreased by 7% at 300°C. According to the results, which is related to the samples without fibers (section 3.4), the fibers have significant impact on the compressive strength, and aramid fibers had the most influence on the results. It is worth mentioning the compressive strength of the specimens without fibers decreased as the temperature increased.

In the samples containing PP and aramid fibers, the compressive strengths developed as the temperature increased. Such an increase could be because of the strengthened cement paste during the evaporation of free water. In fact, the cement gel layers were relocated closer to each other at higher temperatures and made greater Van der Waal's forces (Dias *et al.* 1990, Khoury 2015).

Yu *et al.* (2014) expressed that compressive strength of cement composite having PVA samples increased by 32% and 6% at 200 and 400°C, respectively. However, the compressive strength of

the samples decreased by 32% and 61% after they were exposed to 600 and 800°C, respectively. Sahmaran *et al.* (2011b) detected that the compressive strength of samples reinforced by PVA fibers dropped as the temperature improved from 200 to 800°C. Moreover, Bhat *et al.* (2014) observed that the compressive strength of cement composite containing PVA fibers increased until 200°C, decreased until 300°C, again increased until 400°C, and finally decreased until 600°C. Kelestemur *et al.* (2014) detected that the compressive strength of cement mortars diminished slightly up to heating at 600°C and then a sharp decline occurred exceeding that point. Morsy *et al.* (2012) observed that the compressive strengths of the control and blended cement mortars were improved with temperatures up to 250°C and then declined as the temperature rose up to 800°C.

Moreover, under compressive forces, only the samples containing PP fibers had multiple hairline cracks, which were very fine during failures. The cracks of the specimens under compressive tests are shown in Fig. 3. Fig. 3(e), which is related to the study has been done by Sahmaran *et al.* (2011b), shows crack patterns of the samples having PVA fibers at 600°C.

### 3.2 splitting tensile properties

The average tensile strengths of the samples at three different temperatures of 20, 100 and 300°C are shown in Fig. 4. The maximum average tensile strength at each temperature was achieved for the samples containing aramid fibers. This amount for aramid fibers at 20, 100 and 300°C was equal to 8.31, 7.32 and 4.62 MPa, respectively. Furthermore, the lowest amount of average tensile strength at 20 and 100°C was related to the samples having PP fibers with the value of 5.7 and 4.95 MPa. Finally, the lowest amount of average tensile strength was related to the samples having basalt fibers after exposure to 300°C (i.e., 3.3 MPa).

According to Table 5, as the temperature increased, the average tensile strengths of all the samples diminished. Thus, sub-elevated temperatures have destructive impacts on concrete

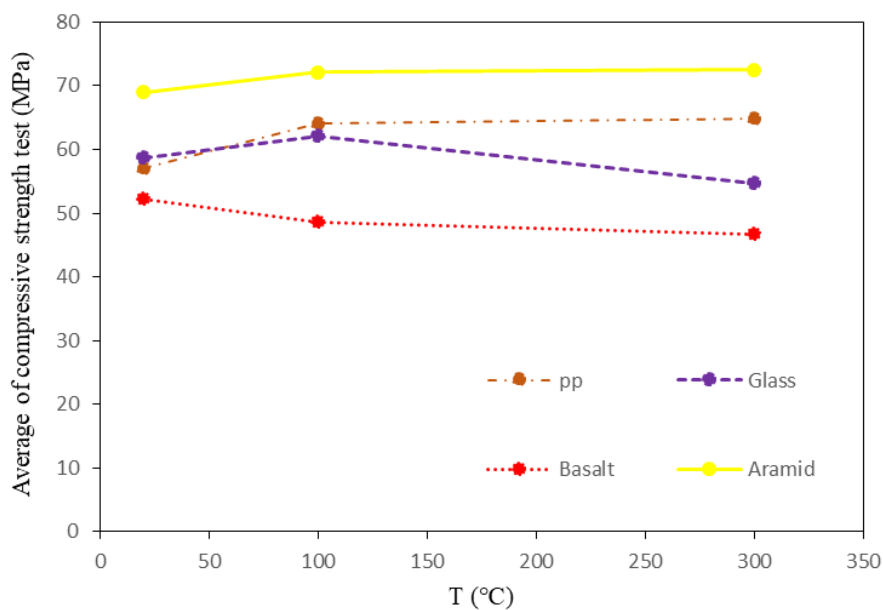


Fig. 2 Effects of the temperature on compressive strength tests

Table 5 Effects of the temperature on tensile strength

Samples	Average tensile strength (MPa)			
	PP fibers	Aramid fibers	Glass fibers	Basalt fibers
20°C	5.7	8.31	6.8	6.34
100°C	4.95	7.32	5.5	5.7
300°C	4.8	4.62	4.6	3.3

specimens, such as decomposing hydration products and destructing the C-S-H gel. In other words, the increase in temperature can reduce the Van der Waal’s forces between C-S-H layers and form Silanol groups (Si-OH: OH-S); therefore, the cracks will increase. Furthermore, sub-elevated temperatures did not significantly affect the average tensile strength of the specimens containing PP fibers, which declined by 13% and 16% at 100 and 300°C, respectively. From the results presented in section 3.4, adding fibers to the mixtures can increase the splitting tensile strength of the samples. Aramid and basalt fibers had the maximum and minimum effects on the splitting

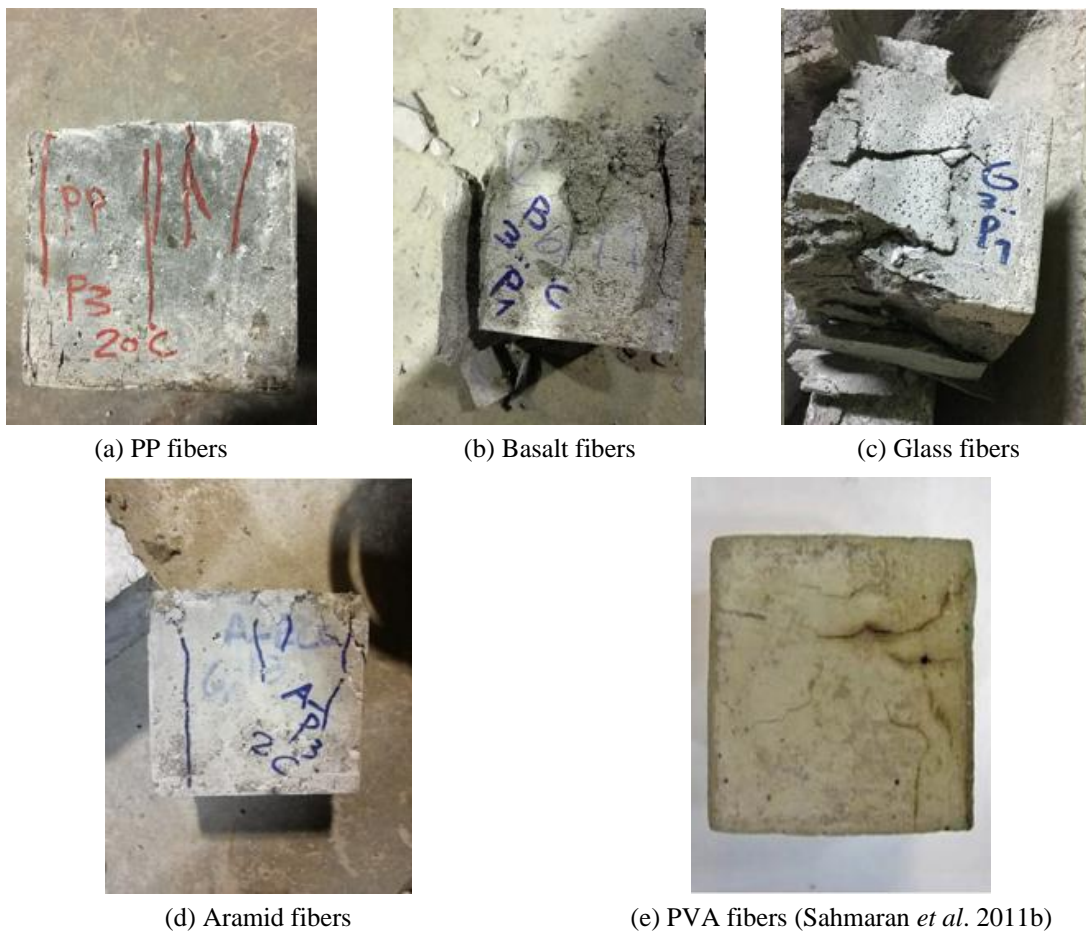


Fig. 3 Cracks of the specimens under compressive strength tests

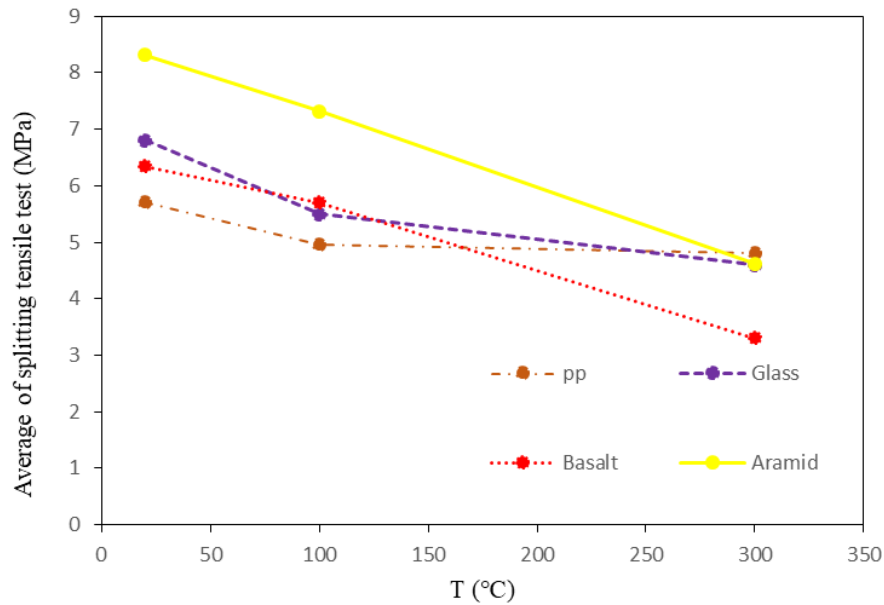


Fig. 4 Effects of the temperature on splitting tensile tests

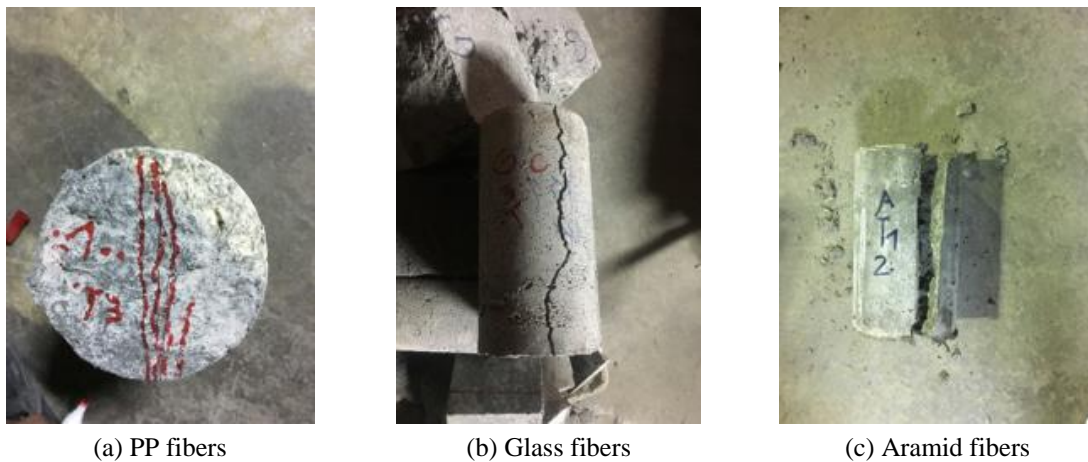


Fig. 5 Cracks of the specimens under splitting tensile tests

tensile test results, which increased them by 45% and 18%, respectively.

These results are in agreement with those reported by Mechtcherine *et al.* (2012), according to whom the tensile strength of the samples diminished at 22, 60, 100 and 150°C. Yu *et al.* (2015) observed that the tensile strength of specimens having high-volume fly ash increased up to 4.07 and 4.91 MPa after exposure to 50 and 100°C, respectively. However, the tensile strength of the samples declined to 3.97 MPa at 200°C. Moreover, Bhat *et al.* (2014) observed that the tensile strength of the samples proliferated by 10% from 20 to 200°C. Afterward, the tensile strength of the specimens declined by 54, 29 and 41% at 300, 400 and 600°C, respectively. Like the



compressive strengths, only the specimens including PP fibers had multiple hairline cracks during failure. The cracks of specimens under splitting tensile tests are shown in Fig. 5.

### 3.3 Flexural properties

The averages of four-point bending tests of the samples at three temperatures of 20, 100, and 300°C are shown in Fig. 6. According to these diagrams, for all three temperatures, the highest amount of the load was related to the specimens having glass fibers before failure. Furthermore, the minimum quantity of the load was related to the samples containing basalt fibers at 20 and 300°C. Also, the samples having PP fibers had the minimum value of the load after exposure to 100°C. The lowest amount of deflection at midspan was related to the samples containing aramid fibers for all three temperatures. As can be seen, the most impacts of adding fibers on the mixes were related to the flexural strength, and the aramid fibers had the maximum influence (50%) on the results. As mentioned above, the addition of fibers in all situations improved the mechanical properties of cement mortars. These results can be explained by the bond strength between the fibers and the cement matrix.

The load decreased for all the samples by increasing the temperature. According to Fig. 6, the samples having PP fibers showed more strain-hardening behavior compared to other samples at 300°C. Moreover, the rate of strain-hardening behavior of the samples decreased by growing the temperature. In agreement with the results of this paper, Du *et al.* (2017) reported that the flexural strength of cement composite having PVA fibers decreased by 22.1, 39.1 and 56.3% at 200, 300 and 400°C, respectively.

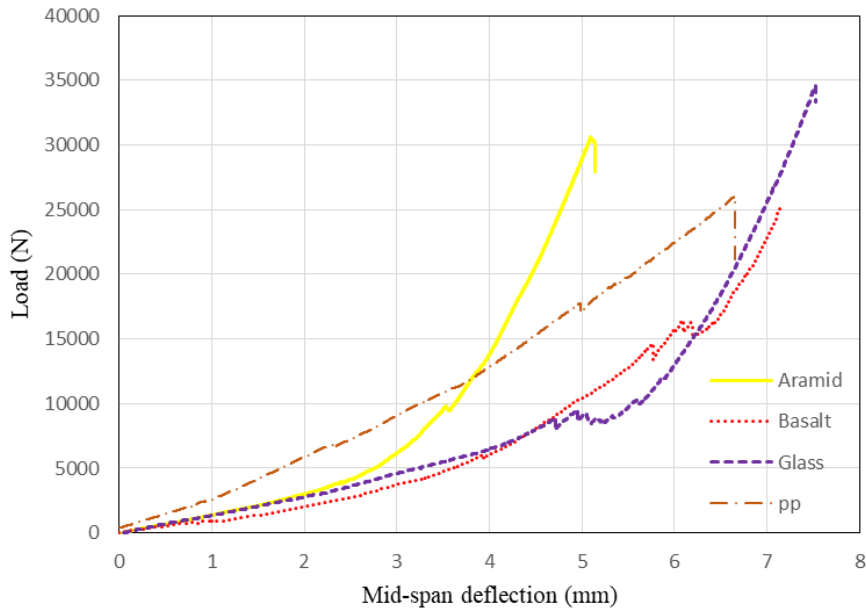
Fig. 6(d), which is related to the study done by Meng *et al.* (2017), shows load-midspan deflection of the samples having PVA fibers. According to this figure, none of the investigated fibers shows enough strain-hardening behavior compared to the PVA.

The results of the average ultimate load, average ultimate flexural strength and mid-span deflection at average ultimate load are summarized in Table 6. The highest value of the average

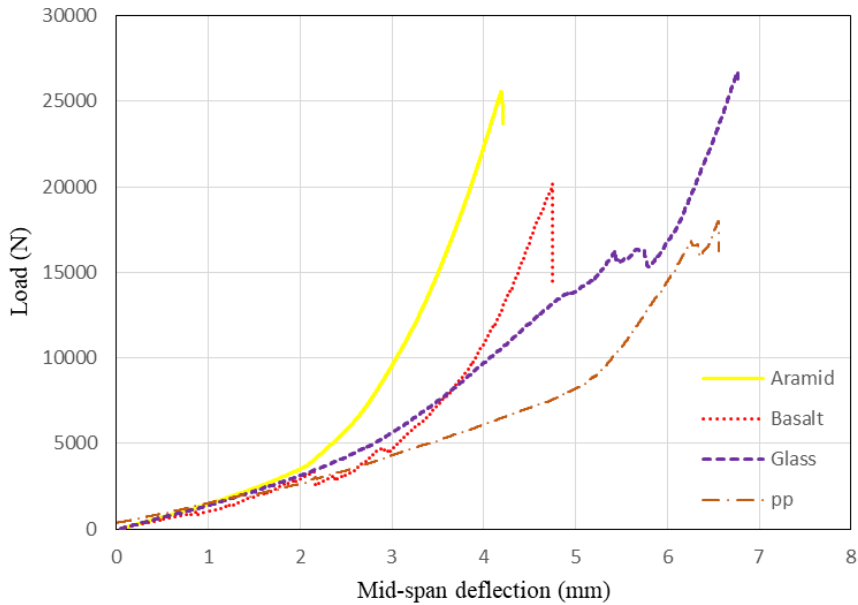
Table 6 Results of average four-point bending tests

Fiber	Average ultimate load (N)	Average ultimate flexural strength (MPa)	Mid-span deflection at average ultimate load (mm)	Temperature (°C)
Aramid	30612.82	9.183	5.09	20
Aramid	25551.81	7.6653	4.19	100
Aramid	15736.01	4.72	3.73	300
Basalt	25306.87	9.915	7.15	20
Basalt	20167.09	6.0501	4.75	100
Basalt	12372.56	3.7116	4.00	300
Glass	34619.62	10.087	7.51	20
Glass	26708.13	8.0124	6.76	100
Glass	17152.59	5.145	4.14	300
PP	26085.52	7.82	6.65	20
PP	17986.73	5.39	6.55	100
PP	16488.76	4.94	4.16	300

ultimate flexural strength is 10.087 MPa (glass fiber), which is higher than of the cement composite containing PVA fibers beams (400 mm × 100 mm × 100 mm) mixed with microsilica sand (8.71 MPa) (Suthiwarapirak *et al.* 2004). The mid-span deflection at the average ultimate load of the aramid, basalt, glass and PP fibers is around 5.09, 7.15, 7.51 and 6.65 mm, respectively. The mid-span deflection ranging for the specimens having PVA fibers using microsilica sand is

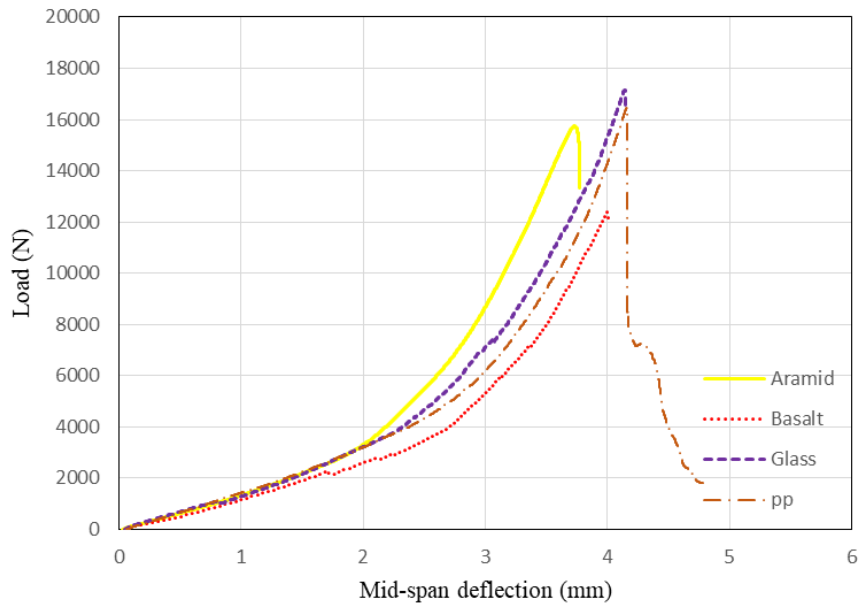


(a) 20°C

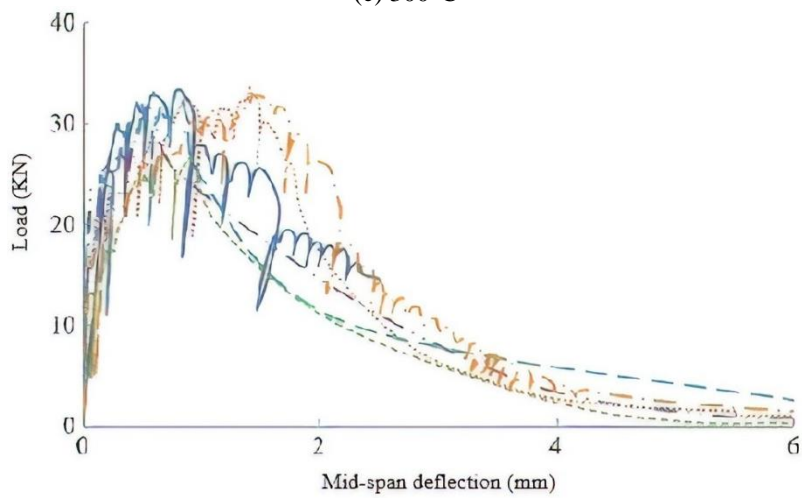


(b) 100°C

Fig. 6 Load-midspan deflection



(c) 300°C



(d) PVA fibers (Meng *et al.* 2017)

Fig. 6 Continued

from 1 to 2 mm (Suthiwarapirak *et al.* 2004). This result shows that the investigated fibers cannot exhibit good deformation capacity. The cracks of specimens under four-point bending tests are presented in Fig. 7. As can be seen in Fig. 7 Single cracks observed at the failure of composites proved.

### 3.4 Specimens without fibers

Table 7 shows mechanical properties of the samples without fibers on average. According to this table in most situations aramid and basalt fibers had maximum and minimum impacts on the

Table 7 Mechanical properties of cement mortars without fibers on average

	Samples without fibers		
	Compressive strength	Splitting tensile strength	Flexural strength
20°C	48	5.5	6
100°C	42	3.9	4.6
300°C	38	2	3.2

mechanical behaviors of cement mortars, respectively. The compressive, splitting tensile and flexural strengths of the samples reinforced with aramid fibers compared to the specimens without fibers increased 43%, 45% and 50 at normal temperature, respectively. Moreover, the compressive, splitting tensile and flexural strengths of the samples having basalt fiber compared to the specimens without fibers increased 8%, 18% and 25% at normal temperature, respectively. As can be seen in this table effects of sub-elevated temperatures on the cement mortars without fibers were considerable.



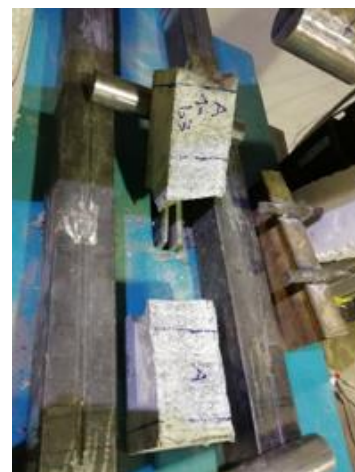
(a) PP fibers



(b) Glass fibers



(c) Basalt fibers



(d) Aramid fibers

Fig. 7 Cracks of the specimens under four-point bending tests

### 3.5 Microstructure of specimens

According to SEM images taken from the specimens, structures of all the samples were homogeneous and condensed. The porosities were generally low in the microstructures of the specimens, which can affect the durability of cement mortars in long run. However, few air pores can be seen in some specimens such as those containing glass fiber (Fig. 8(b)). All images in Fig. 8 show that the amounts of calcium hydroxide crystals are very low; therefore, the specimens should have acceptable mechanical properties. In fact, silica fume is a pozzolan that converts calcium hydroxide into calcium-silicate-hydrate (C-S-H) gel (Mazloom *et al.* 2018b, Afzali Naniz and Mazloom 2018). In this research, the percentage of silica fume in the mixes was 15%, which was quite high and enough for consuming Calcium Hydroxide.

Physical interlayer water evaporates at 120°C while chemical water evaporates at 180°C to 300°C (Othuman and Wang 2011). Thus, sub-elevated temperatures have destructive impacts on concrete specimens, such as decomposing hydration products and destructing the C-S-H gel. In other words, temperature rise can reduce the Van der Waal's forces between C-S-H layers and form Silanol groups (Si-OH: OH-S); leading to an increase in the number of created cracks. In this study, the destructive impacts of temperature rise on tensile and four-point bending tests are noticeably observed. For example, in Figs. 9(d), (e) and (f), which are related to specimens having basalt fibers, numerous cracks are formed in the microstructures by the increase in temperature and the

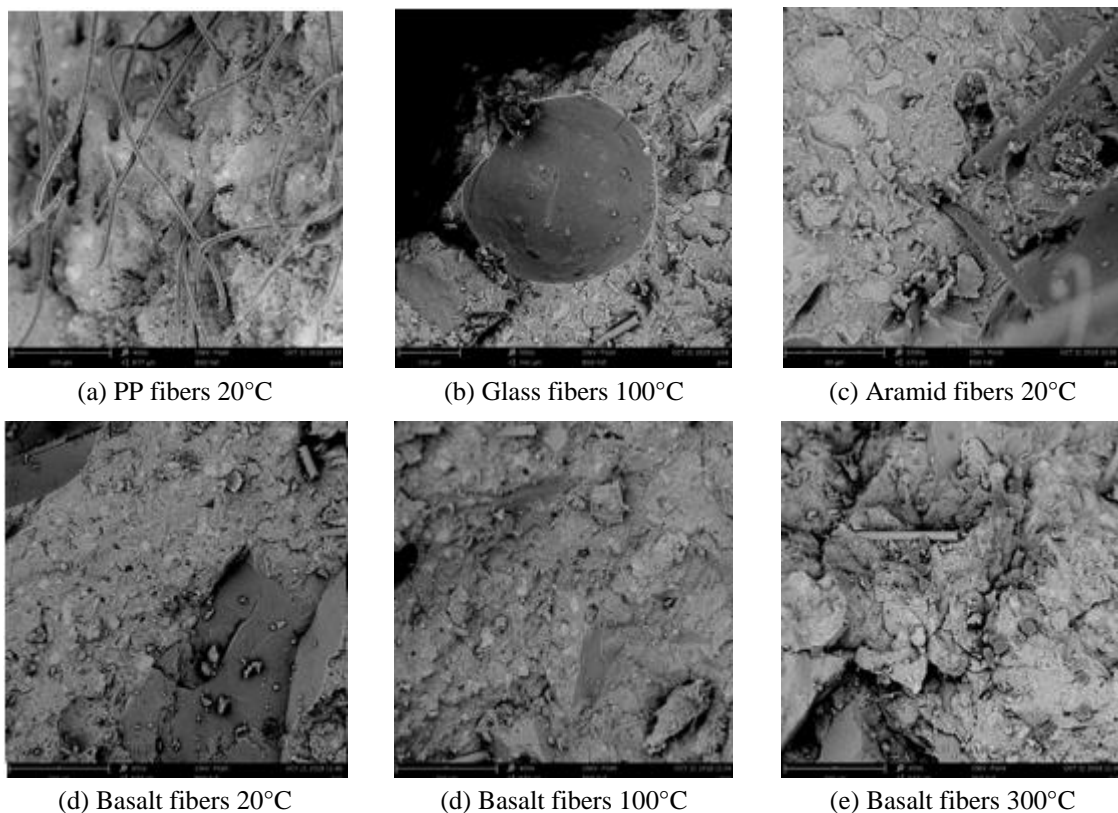


Fig. 8 Microstructures of the specimens at different temperatures

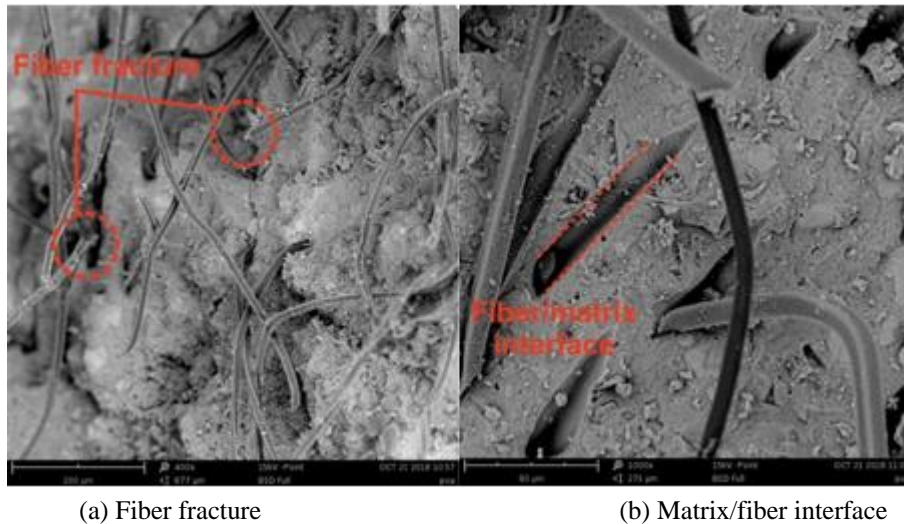


Fig. 9 PP fiber and matrix/fiber interface

destruction of C-S-H gel.

In the specimens having PP and aramid fibers, the compressive strengths improved with a temperature raised. This result can be explained by strengthened cement paste during the evaporation of free water. In fact, the cement gel layers relocated closer to each other at higher temperatures and made greater Van der Waal's forces (Dias *et al.* 1990, Khoury 2015). Furthermore, the hydration of cement particles, which have not participated in the hydration process before reaching this temperature, can be considered as another mechanism in this regard (Morsy *et al.* 2012). In other words, transferring water among the pores at sub-elevated temperatures may cause the cement pastes to hydrate. Actually, the high water absorption of PP and aramid fibers compared to those of basalt and glass fibers probably is the main reason for having higher water content to move and higher compressive strength.

According to the microstructures of the specimens presented in Fig. 8, it is seen that the distribution of PP fibers was more suitable than the other ones. Fig. 9 shows that in most situations, the bond strength between the PP fibers and the cement matrix was adequate; therefore, the fibers did not pull out the matrix, and they ruptured.

#### 4. Conclusions

The main goals of this research are to investigate the thermal effects on the mechanical properties of cement mortars reinforced with aramid, glass, basalt and polypropylene fibers. For this purpose, all the samples had the same mix proportions, and only their fiber types were different. Based on the results presented in this paper, it can be concluded that:

- According to the test results, the fiber type did not have considerable effects on the mechanical properties of the samples at sub-elevated temperatures. In other words, using the fibers with higher melting points could not improve the qualities of the samples in sub-elevated temperatures.

- The effects of sub-elevated temperatures on the splitting tensile strength and four-point bending tests of different samples were studied in this research. The negative effects of sub-elevated temperatures on four-point bending tests were much more than the others. In fact, the splitting tensile strengths of the samples decreased about 14% and 35% in average at 100°C and 300°C, respectively. Moreover, the bending strengths of the specimens diminished about 27% and 49% in average at 100°C and 300°C, respectively.
- The tensile to the compressive strength ratios of the samples decreased about 31% and 41% in average at 100°C and 300°C, respectively. The reason for this result was the increase in the numerous cracks observed in the microstructures of the specimens at sub-elevated temperatures.
- The samples containing aramid, basalt, glass and polypropylene (PP) fibers showed some strain-hardening behaviors, and the PP ones were better than the others in some situations. In fact, they behave similar to fiber-reinforced cementitious composite (FRCC). It is worth emphasizing that the aspect ratios ( $L_f/d_f$ ) of the fibers were high enough.
- According to SEM images taken from the samples, the bond strength between the PP fibers and the cement matrix was higher than those of the other fibers. In this regard, only the specimens having PP fibers among the investigated fibers had multiple hairline cracks.
- The four-point bending tests were the most suitable ones to check the strain-hardening behavior of the specimens. According to these tests, the samples containing PP fibers should have more than 2% volumetric percentages of the mixture to show appropriate strain-hardening behavior.

## Acknowledgments

This work was supported by Shahid Rajaei Teacher Training University.

## References

- Afzali Naniz, O. and Mazloom, M. (2018), "Effects of colloidal nano-silica on fresh and hardened properties of self-compacting lightweight concrete", *J. Build. Eng.*, **20**, 400-410.  
<https://doi.org/10.1016/j.jobbe.2018.08.014>
- Afzali Naniz, O. and Mazloom, M. (2019), "Assessment of the influence of micro- and nano-silica on the behavior of self-compacting lightweight concrete using full factorial design", *Asian J. Civil Eng.*, **20**, 57-70. <https://doi.org/10.1007/s42107-018-0088-2>
- ASTM C1609/M-05 (2006), Standard Test Method for Flexural Performance of Fiber Reinforced Concrete (using Beam with Third-point loading), West Conshohocke, PA, USA.
- Bhat, P.S., Chang, V. and Li, M. (2014), "Effect of elevated temperature on strain-hardening engineered cementitious composites", *Constr. Build. Mater.*, **69**, 370-380.  
<https://doi.org/10.1016/j.conbuildmat.2014.07.052>
- BS 1881: part 108. (1983a), Method for making test cubes from fresh concrete.
- BS 1881: part 111. (1983b), Method of testing concrete.
- BS 1881: part 117. (1983c), Method for determination of tensile splitting strength.
- Dias, W.P.S., Khoury, G.A. and Sullivan, P.J.E. (1990), "Mechanical properties of hardened cement paste exposed to temperatures up to 700°C (1292°F)", *ACI Mater.*, **87**, 160-166.
- Du, Q., Wei, J. and Lv, J. (2017), "Effects of High Temperature on Mechanical Properties of Polyvinyl Alcohol Engineered Cementitious Composites", *Int. J. Civ. Eng.*, **16**(8), 965-972.  
<https://doi.org/10.1007/s40999-017-0245-0>

- Karamloo, M., Mazloom, M. and Payganeh, G. (2017), "Effect of size on nominal strength of self-compacting lightweight concrete and self-compacting normal weight concrete: A stress-based approach", *Mater. Today Commun.*, **13**, 36-45. <https://doi.org/10.1016/j.mtcomm.2017.08.002>
- Kelestemur, O., Arıcı, E., Yıldız, S. and Gokcer, B. (2014), "Performance evaluation of cement mortars containing marble dust and glass fiber exposed to high temperature by using Taguchi method", *Constr. Build. Mater.*, **60**, 17-24. <https://doi.org/10.1016/j.conbuildmat.2014.02.061>
- Khoury, G.A. (2015), "Compressive strength of concrete at high temperatures: a reassessment", *Mag. Concrete Res.*, **161**, 291-309. <https://doi.org/10.1680/mac.1992.44.161.291>
- Li, V.C. (1998), "Engineered Cementitious Composites - Tailored Composites Through Micromechanical Modeling Fiber Reinforced Concrete: Present and the Future edited by N. Banthia, in Fiber Reinforced Concrete", (Present and the Future edited by N. Banthia, A. Bentur, A. and A. Mufti), Canadian Society for Civil Engineering, Montreal, Canada, pp. 64-97.
- Li, V.C. (2000), "Strategies for high performance fiber reinforced cementitious composites development", *Proceedings of International Workshop on Advances in Fiber Reinforced Concrete*, Bergamo, Italy, pp. 93-98.
- Li, V.C. (2003), "On engineered cementitious composites (ECC): A review of the material and its applications", *Adv. Concrete Tech.*, **1**(3), 215-230. <http://hdl.handle.net/2027.42/84703>
- Li, V.C. (2007), "Engineered Cementitious Composites (ECC) – Material, Structural, and Durability Performance".
- Li, V.C. (2008), "Durability of mechanically loaded engineered cementitious composites under highly alkaline environments", **30**, 72-81. <https://doi.org/10.1016/j.cemconcomp.2007.09.004>
- Li, V.C. (2012), "Tailoring ECC for Special Attributes", *Int. J. Concr. Struct. Mater.*, **6**, 135-144. <https://doi.org/10.1007/s40069-012-0018-8>
- Li, V.C. (2017), "From Micromechanics to Structural Engineering - The Design of Cementitious Composites for Civil Engineering Applications".
- Li, V.C., Wu, H.C., Maalej, M.D. and Mishra, D. (1996), "Tensile behavior of cement-based composite with random discontinuous steel fibers", *J. Am. Ceram. Soc.*, **79**, 74-78.
- Li, V.C., Wu, C., Wang, S. and Ogawa, A. (2002), "Interface tailoring for strain-hardening polyvinyl alcohol-engineered cementitious composites (PVA-ECC)", *ACI Mater.*, **99**(5), 463-472.
- Maalej, M., Quek, S.T. and Zhang, J. (2005), "Behavior of hybrid-fiber engineered cementitious composites subjected to dynamic tensile loading and projectile impact", **17**, 143-152. [https://doi.org/10.1061/\(ASCE\)0899-1561\(2005\)17:2\(143\)](https://doi.org/10.1061/(ASCE)0899-1561(2005)17:2(143))
- Mazloom, M. (2008), "Estimating long-term creep and shrinkage of high-strength concrete", *Cem. Concrete Compos.*, **30**(4), 316-326. <https://doi.org/10.1016/j.cemconcomp.2007.09.006>
- Mazloom, M. and Mahboubi, F. (2017), "Evaluating the settlement of lightweight coarse aggregate in self-compacting lightweight concrete", *Comput. Concrete, Int. J.*, **19**(2), 203-210. <https://doi.org/10.12989/cac.2017.19.2.203>
- Mazloom, M. and Miri, M.S. (2017), "Interaction of magnetic water, silica fume and superplasticizer on fresh and hardened properties of concrete", *Adv. Concrete Constr., Int. J.*, **5**(2), 87-99. <https://doi.org/10.12989/acc.2017.5.2.087>
- Mazloom, M. and Ranjbar, A. (2010), "Relation between the workability and strength of self-compacting concrete", *Proceedings of the 35th Conference on Our World in Concrete & Structures*, Singapore, pp. 315-322.
- Mazloom, M. and Yoosefi, M.M. (2013), "Predicting the indirect tensile strength of self-compacting concrete using artificial neural networks", *Comput. Concrete, Int. J.*, **12**(3), 285-301. <https://doi.org/10.12989/cac.2013.12.3.285>
- Mazloom, M., Ramezani-pour, A.A. and Brooks, J.J. (2004), "Effect of silica fume on mechanical properties of high-strength concrete", *Cem. Concrete Compos.*, **26**(1), 347-357. [https://doi.org/10.1016/S0958-9465\(03\)00017-9](https://doi.org/10.1016/S0958-9465(03)00017-9)
- Mazloom, M., Saffari, A. and Mehrvand, M. (2015), "Compressive, shear and torsional strength of beams made of self-compacting concrete", *Comput. Concrete, Int. J.*, **15**(6), 935-950.



- <https://doi.org/10.12989/cac.2015.15.6.935>
- Mazloom, M., Allahabadi, A. and Karamloo, M. (2017), "Effect of silica fume and polyepoxide-based polymer on electrical resistivity", *Adv. Concrete Constr., Int. J.*, **5**(6), 587-611.  
<https://doi.org/10.12989/acc.2017.5.6.587>
- Mazloom, M., Homayooni, S.M. and Miri, S.M. (2018a), "Effect of rock flour type on rheology and strength of self-compacting lightweight concrete", *Comput. Concrete, Int. J.*, **21**(2), 199-207.  
<https://doi.org/10.12989/cac.2018.21.2.199>
- Mazloom, M., Soltani, A., Karamloo, M., Hasanloo, A. and Ranjbar, A. (2018b), "Effects of silica fume, superplasticizer dosage and type of superplasticizer on the properties of normal and self-compacting concrete", *Adv. Mater. Res., Int. J.*, **7**(1), 407-434. <https://doi.org/10.12989/amr.2018.7.1.045>
- Mechtcherine, V., Andrade, F.De., Müller, S.P., Jun, P., Dias, R. and Filho, T. (2012), "Cement and Concrete Research Coupled strain rate and temperature effects on the tensile behavior of strain-hardening cement-based composites (SHCC) with PVA fibers", *Cem. Concrete Res.*, **42**, 1417-1427.  
<https://doi.org/10.1016/j.cemconres.2012.08.011>
- Meng, D., Huang, T., Zhang, Y.X. and Lee, C.K. (2017), "Mechanical behavior of a polyvinyl alcohol fiber reinforced engineered cementitious composite (PVA-ECC) using local ingredients", *Constr. Build. Mater.*, **141**, 259-270.
- Morsy, M.S., Abbas, H. and Alsayed, S.H. (2012), "Behavior of blended cement mortars containing nano-metakaolin at elevated temperatures", *Constr. Build. Mater.*, **35**, 900-905.  
<https://doi.org/10.1016/j.conbuildmat.2012.04.099>
- Othuman, A. and Wang, Y.C. (2011), "Elevated-temperature thermal properties of lightweight foamed concrete", *Constr. Build. Mater.*, **25**, 705-716. <https://doi.org/10.1016/j.conbuildmat.2010.07.016>
- Qian, S. and Li, V.C. (2007), "Simplified Inverse Method for Determining the Tensile Strain Capacity of Strain Hardening Cementitious Composites", *Adv. Concrete Tech.*, **5**, 235-246.  
<https://doi.org/10.3151/jact.5.235>
- Sahmaran, M. and Li, V.C. (2007), "De-icing salt scaling resistance of mechanically loaded engineered cementitious composites", *Cement Concrete Res.*, **37**, 1035-1046.  
<https://doi.org/10.1016/j.cemconres.2007.04.001>
- Şahmaran, M., Lachemi, M. and Li, V.C. (2010), "Assessing mechanical properties and microstructure of fire-damaged engineered cementitious composites", *ACI Mater.*, **107**(3), 297-304.
- Sahmaran, M., Li, M. and Li, V.C. (2011a), "Transport properties of engineered cementitious composites under chloride exposure", *ACI Mater J.*, **104**(6), p. 604.
- Şahmaran, M., Özbay, E., Yücel, H.E., Lachemi, M. and Li, V.C. (2011b), "Effect of fly ash and PVA fiber on microstructural damage and residual properties of engineered cementitious composites exposed to high temperatures", *J. Mater. Civil Eng.*, **23**, 1735-1745.  
[https://doi.org/10.1061/\(ASCE\)MT.1943-5533.0000335](https://doi.org/10.1061/(ASCE)MT.1943-5533.0000335)
- Salehi, H. and Mazloom, M. (2018), "Effect of magnetic-field intensity on fracture behaviors of self-compacting lightweight concrete", *Mag. Concr. Res.*, **71**(13), 665-679.  
<https://doi.org/10.1680/jmacr.17.00418>
- Salehi, H. and Mazloom, M. (2019a), "Opposite effects of ground granulated blast-furnace slag and silica fume on the fracture behavior of self-compacting lightweight concrete", *Constr. Build. Mater.*, **222**, 622-632. <https://doi.org/10.1016/j.conbuildmat.2019.06.183>
- Salehi, H. and Mazloom, M. (2019b), "An experimental investigation on fracture parameters and brittleness of self-compacting lightweight concrete containing magnetic field treated water", *Arch. Civil Mech. Eng.*, **19**, 803-819. <https://doi.org/10.1016/j.acme.2018.10.008>
- Sirijaroonchai, K., El-tawil, S. and Parra-montesinos, G. (2010), "Behavior of high performance fiber reinforced cement composites under multi-axial compressive loading", *Cem. Concrete Compos.*, **32**, 62-72.  
<https://doi.org/10.1016/j.cemconcomp.2009.09.003>
- Suthiwarapirak, P., Matsumoto, T. and Kanda, T. (2004), "Multiple cracking and fiber bridging characteristics of engineered cementitious composites under fatigue flexure", *J. Mater. Civil Eng.*, **16**, 433-443. [https://doi.org/10.1061/\(ASCE\)0899-1561\(2004\)16:5\(433\)](https://doi.org/10.1061/(ASCE)0899-1561(2004)16:5(433))

- Yang, E. and Li, V.C. (2010), "Strain-hardening fiber cement optimization and component tailoring by means of a micromechanical model". *Constr. Build. Mater.*, **24**, 130-139.  
<https://doi.org/10.1016/j.conbuildmat.2007.05.014>
- Yang, E., Wang, S., Yang, Y. and Li, V.C. (2008), "Fiber-bridging constitutive law of engineered cementitious composites", *Adv. Concrete Tech.*, **6**, 181-193. <https://doi.org/10.3151/jact.6.181>
- Yang, E.H., Sahmaran, M., Yang, Y. and Li, V.C. (2009), "Rheological control in production of engineered cementitious composites", *ACI Mater.*, **106**(4), 357-366.
- Yu, J., Weng, W. and Yu, K. (2014), "Effect of different cooling regimes on the mechanical properties of cementitious composites subjected to high temperatures", *Sci. World J.*  
<http://dx.doi.org/10.1155/2014/289213>
- Yu, J., Lin, J., Zhang, Z. and Li, V.C. (2015), "Mechanical performance of ECC with high-volume fly ash after sub-elevated temperatures", *Constr. Build. Mater.*, **99**, 82-89.  
<https://doi.org/10.1016/j.conbuildmat.2015.09.002>
- Yu, K.Q., Yu, J.T., Dai, J.G., Lu, Z.D. and Shah, S.P. (2018), "Development of ultra-high performance engineered cementitious composites using polyethylene (PE) fibers", *Constr. Build. Mater.*, **158**, 217-227.  
<https://doi.org/10.1016/j.conbuildmat.2017.10.040>
- Zhang, J., Wang, Z., Ju, X. and Shi, Z. (2014), "Simulation of flexural performance of layered ECC-concrete composite beam with fracture mechanics model", *Eng. Fract. Mech.*, **131**, 419-438.  
<https://doi.org/10.1016/j.engfracmech.2014.08.016>